X-ray absorption spectroscopy on solid krypton up to 20 GPa

A. Polian and J. P. Itie
Laboratoire de Physique des Milieux Condensés, Université Pierre et Marie Curie, T13 E4, 4 place Jussieu, F-75252 Paris CEDEX 05, France

E. Dartyge, A. Fontaine, and G. Tourillon
Laboratoire pour l'Utilisation du Rayonnement Electromagnétique, Université de Paris–Sud, Bâtiment 209D, F-91405 Orsay CEDEX, France
(Received 27 July 1988)

High-pressure properties of krypton were investigated by energy-dispersive extended x-ray absorption fine-structure spectroscopy in a diamond anvil cell at room temperature. The equation of state agrees very well with x-ray diffraction data. The pressure dependence of the Debye-Waller factor was determined and compared with calculations using pair potentials. The analysis of the x-ray absorption near-edge structure part of the spectrum shows the possibility of measuring the pressure in bubbles of krypton implanted in metallic matrices.

INTRODUCTION

Because of the spherical electronic shells of their constituent atoms rare-gas solids (RGS) are the best candidates for use in comparing experimental results with theoretical predictions using various interaction potentials. The study of RGS is also interesting for a better understanding of giant planets of the solar system.

Among optical techniques currently used to study materials at high density, only a few are applicable to RGS, which generally crystallize in a face-centered-cubic (fcc) structure and are Raman and infrared inactive. X-ray diffraction[1–4] and Brillouin scattering[5–7] are the most commonly used techniques in studying RGS; Brillouin scattering determines the elastic constants and x-ray diffraction leads to the equation of state (EOS).

X-ray absorption spectroscopy (XAS), particularly the extended x-ray absorption fine-structure (EXAFS) spectroscopy, gives information about the interatomic distances and their mean-square deviation (Debye-Waller factor) as well as the coordination number. XAS has been shown to be sensitive to pressure,[8–12] giving information about equations of state, local compressibility, and the pressure dependence of the Debye-Waller factor.

The aim of this paper is to present XAS results obtained on solid krypton up to 20 GPa and to compare the EOS obtained from the EXAFS results with the EOS obtained from x-ray diffraction.

The pressure dependence of the x-ray absorption near-edge structure (XANES) has also a great interest for the understanding of XAS data obtained on krypton bubbles implanted in metallic matrices.

EXPERIMENT

The experiments were carried out at the energy dispersive XAS port at Laboratoire Pour l'Utisation du Rayonnement Electromagnétique (LURE) (Orsay, France). The characteristics of the spectrometer are described elsewhere.[13,14] For high-pressure experiments, the main advantages of this setup are as follows.

(i) The beam is focused. The focus size was about 1 mm with the triangle shaped crystal, and less than 500 μm for the newly cut crystal which achieved a shape close to the optimized ellipsoid.

(ii) The entire spectrum is obtained at once in a short time (about 1 s) which makes the alignment much easier.

(iii) There is no mechanical movement, so that the crucial alignment of the pressure cell with respect to the sample which is 200 μm in diameter is maintained. The high-pressure cell was a classical Block and Piermarini[15] diamond anvil cell, cryogenically[5] loaded with krypton. The pressure was measured outside the hutch, using the power-of-five-law ruby-fluorescence scale.[16]

In this experiment the x-ray beam goes through the diamond anvils. Using this geometry, any type of diamond anvil cell can be used, with a stainless steel or Inconel gasket. The main disadvantage is that one may obtain some extra absorptionlike peaks, so-called "glitches," due to Bragg reflections by the monocrystalline anvils.[17] A Bragg reflection deviates photons of a given energy out of the beam path which consequently do not fall on the detector resulting in extra localized absorptionlike peaks in the spectra. The extra peaks may strongly perturb the EXAFS or XANES spectra. A motor-driven stage is used in order to rotate the cell and thus shift the diamond Bragg peaks as far away as possible from the absorption edge of interest (with the dispersive mode, the whole spectrum is obtained at once, which makes this adjustment easier).

We measured the absorption spectrum of solid krypton at the krypton K edge (14 385 eV). It takes 3.5 s to collect the 1024 data of one spectrum. In order to improve the signal-to-noise ratio, 160 spectra were added together. If we include the measurement of the fixed-pattern signal which can be subtracted because of its stability

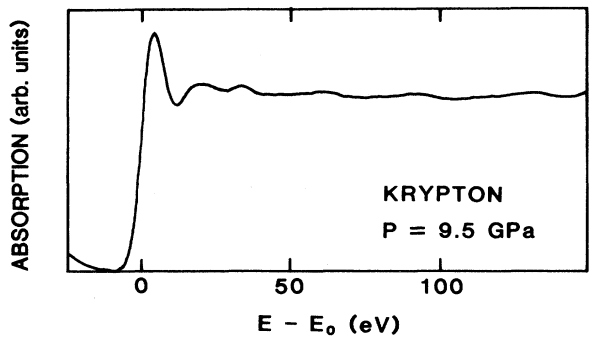

FIG. 1. Absorption spectrum at 9.5 GPa after regular processing. The usable energy is about 150 eV above the edge. Due to the high value of the lattice parameter, there are five oscillations in that energy range.

with respect to time, the real data collection time is doubled. Thus the overall time used to record one spectrum is 20 min.

The readout of the photodiode array gives a signal per pixel. It is necessary to assign an energy value for each pixel. In order to get this energy calibration of the collected spectra, measurements of known standards are made and compared to data collected using step-by-step scans. The standard spectra contain energy scales derived from knowledge of the absolute values of the Bragg angle. For this experiment, the energy calibration of the photodiode array has been carried out by the measurement of the spectra of a Au-Cu sample at the Au $L1$ edge.

Because of the small size of the krypton sample in the diamond anvil cell ($\phi \sim 200$ μm), only a part of the beam ($\phi \sim 1$ mm) is usable. This reduces the energy range available to 150 eV above the absorption edge for this experiment. The threshold energy is taken at the inflection point of the edge (Fig. 1).

RESULTS AND DISCUSSION

The oscillatory part of the absorption coefficient for a cubic crystal is given by

$$\chi(k)=\frac{\mu-\mu_0}{\mu_0} ,$$

where μ_0 is the atomiclike cross section and μ the measured one.

Using the one electron, single-scattering approximation

$$\chi(k)=-\sum_j \frac{N_j}{kR_j^2}|f_j(k,\pi)|\sin[2\mathbf{k}\cdot\mathbf{R}_j+\Psi_j(k)] \times e^{-2\sigma_j^2 k^2} e^{-2R_j/\lambda_j(k)} , \quad (1)$$

where N_j is the number of neighbor atoms at a distance R_j, $|f_j(k,\pi)|$ the backscattering amplitude, $\lambda_j(k)$ the electron mean free path, σ_j^2 the mean-square displacement between the absorbing atom and the jth backscattering atom (the so-called Debye-Waller factor) and $\Psi_j(k)$ the total phase shift due to the backscattering and absorbing atoms.

The photoelectron wave vector k is given by

$$k=\hbar^{-1}[2m(E-E_0)]^{1/2} , \quad (2)$$

where E is the energy of the incident x-ray photon and E_0 the threshold energy. Those expressions mean that the essential function of the photon is to create a photoelectron from one krypton atom. Then, the spherical electronic wave is partly backscattered by the neighbors and the final state of the dipolar transition is essentially a superposition of the outgoing wave and the backcoming wavelets, resulting in interferences. When the kinetic energy of the photoelectron is small, the mean free path is much longer. Thus, more than a single scattering may be necessary to achieve a good description of the final state; it is the XANES range which is approximatively limited to 50 eV above the absorption edge.

The $\chi(k)$ is extracted by substracting the base line obtained by a smoothing method and is shown, for example, at 9.5 GPa, in Fig. 2. To get information in the R space, a Fourier transform of the $k^n\chi(k)$ data must be made. In the present case, we used $n=1$. We must point out that in this experiment we have not been able to collect data over a wide energy range compared to that which is used in a regular experiment. However, the number of oscillations of our spectra is large enough to get a very significant signal. For each pressure, we took care to use the same window for the Fourier-transform procedure. The Fourier transform spectrum at 9.5 GPa is shown in Fig. 3. The large peak around 3.5 Å is the contribution of the shell of the 12 first neighbors.

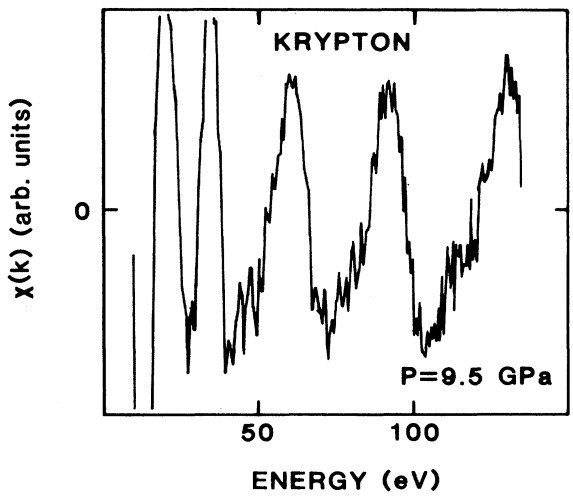

FIG. 2. EXAFS oscillations at 9.5 GPa as a function of the energy distance from the threshold energy.

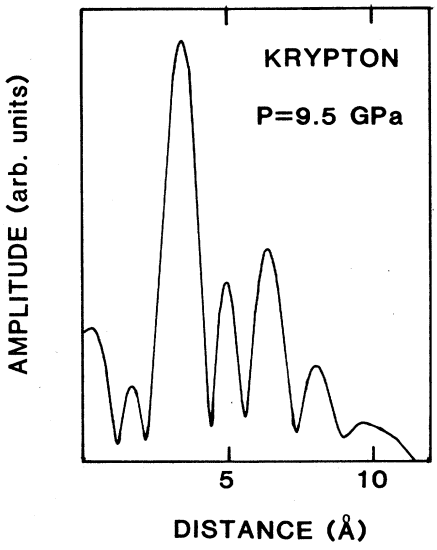

FIG. 3. Fourier transform of the EXAFS oscillations at $P=9.5$ GPa. The largest peak is due to the 12 first neighbors of the close-packed solid.

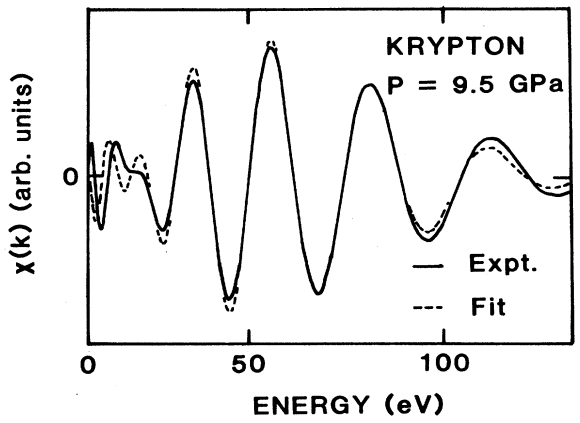

FIG. 4. Inverse Fourier transform of the first-neighbors peak (continuous line) compared with calculated EXAFS oscillations giving the best fit.

In order to determine the nearest-neighbor interatomic distance R and the Debye-Waller factor σ, the following procedure was used.

First, it is necessary to know for a pair of krypton atoms, the backscattering amplitude $|f_j(k)|$ and the phase shift $\Psi_j(k)$, which are assumed to be pressure independent. This is a common requirement of the EXAFS data analysis. The general and precise method of solving this problem is to extract this information from the spectra of well-known samples. In the present case, this has been obtained from the spectrum at 15.7 GPa, where R was determined by x-ray diffraction[7] and σ chosen arbitrarily to be 0. The choice of the Debye-Waller factor at 15.7 GPa is not obvious. There is no known case in which the backscattering amplitude for a sample has allowed an absolute determination of σ. Thus only variation of σ^2 are significant. Hence, the procedure followed incorporates the Debye-Waller factor as a contribution in the amplitude of the signal at 15.7 GPa. The two parameters, $|f_j(k)|$ and $\Psi_j(k)$, are adjusted in order to fit the $\chi(k)$ calculated using Eq. (1) to the inverse Fourier transform (IFT) of the first-neighbor peak.

Second, for each pressure, using the values of $|f_j(k)|$ and $\Psi_j(k)$ obtained previously, the calculated $\chi(k)$ was fitted to the IFT of the first-neighbor peak, with two adjustable parameters R and σ. Such a fit is shown in Fig. 4. In this figure the solid line represents the IFT, labeled "experimental," and the dashed line is the best fit.

Examples of the evolution of the absorption spectra with pressure are shown in Fig. 5. First, a strong white line is observed, even at low pressure. This white line does not exist in the gas phase[18] and so cannot be assigned to the Rydberg states. On the contrary, pressure generally broadens similar states like excitons in solid.[19] Another noticeable feature is the increase of the amplitude of the EXAFS oscillations. At 1.6 GPa, which is far above the melting pressure (about 0.7 GPa at 300 K), the oscillations are so weak that the spectrum is useless for deducing the interatomic distances. Fortunately the thermal motion of the atoms is reduced dramatically when the pressure increases. This point will be discussed below.

The lattice parameter obtained from the present EXAFS measurements is compared with the x-ray diffraction data[7] in Fig. 6. In this figure the stars represent the EXAFS results and the squares the diffraction ones. Good agreement between both set of data is observed. This is not quite true in the low-pressure range where EXAFS data give lower values than the x-ray diffraction. This is a general finding of EXAFS when the distance distribution starts to be too broad, as

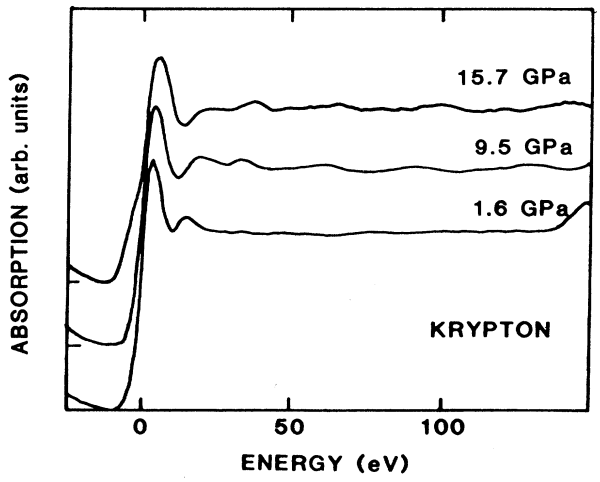

FIG. 5. Example of evolution of the absorption spectrum as a function of the pressure.

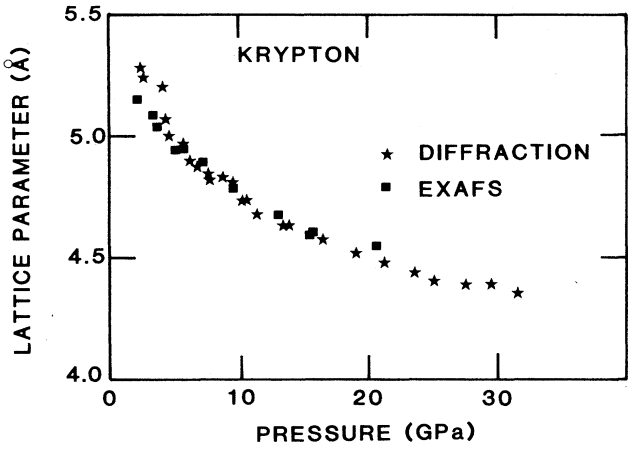

FIG. 6. Comparison of the pressure dependence of the lattice parameter determined by x-ray diffraction (squares) and EXAFS (stars).

demonstrated by Eisenberger and Brown on pure zinc.[20] The harmonic analysis of the thermal motion becomes inaccurate and it is no longer possible to restrict the real distribution to its two momenta (order 1, average distance; order 2, Debye-Waller factor). EXAFS imposes even more constraints than diffraction data because of the $1/R^2$ geometrical factor and the $e^{-\lambda R}$ inelastic factor in the overall amplitude which reshape the real distribution.

EXAFS data allow the determination of only a change in the Debye-Waller factor. The classical method is to take the zero-pressure room-temperature value as a reference. Since, under this condition, krypton is a gas, the change in the Debye-Waller factor was measured using 15.7 GPa as a starting point.

The thermal contribution to the Debye-Waller factor σ_t is determined by the mean-square displacement of the central absorbing atom relative to its neighbors,

$$\sigma_t^2 = \langle (\mathbf{u}_i - \mathbf{u}_j)\cdot\mathbf{R}_{ij} \rangle \ , \tag{3}$$

where $\mathbf{u}_i$ is the displacement from the equilibrium position of the atom i and $\mathbf{R}_{ij}$ is a unit vector in the direction ij, the bracket indicating the thermal average. Using the self-consistent harmonic theory plus a cubic anharmonic term,[21] Loubeyre calculated the mean displacement amplitude of the phonons in krypton[22] as a function of the pressure, using Aziz's Hartree-Fock plus dispersion-pair potential.[23] Results of these calculations are shown in Fig. 7 (points).

In order to compare these calculations with experiment, and because the experimental value is only a relative value, a constant value of 0.0069 Å^2 (calculated value of σ^2 at 15.7 GPa) was added to the experimental results (stars in Fig. 7). The comparison shows the remarkable agreement between the shifted experimental values and calculated results. The very fast variation of σ^2 with pressure at low pressure relates to the approach of melting and to the weak van der Waals interatomic potential: 1.5 GPa above melting, the mean-square displacement corresponds to an amplitude of about 10% of the first-neighbor distance.

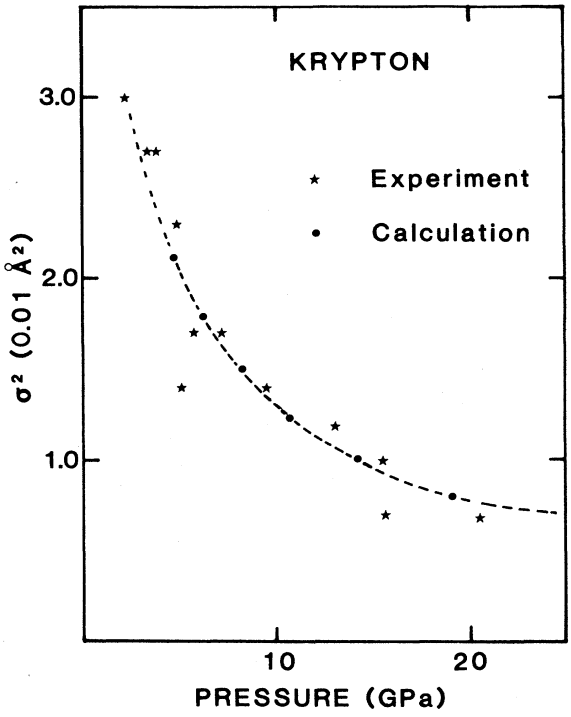

FIG. 7. Experimental (stars) and calculated (points) Debye-Waller factor. Reference for the experiments is taken at $P = 15.7$ GPa. All the experimental points are then shifted by a constant value (see text).

It should be noticed here that the calculations are done using true pair potentials; $\langle u^2 \rangle$ is not sensitive to many

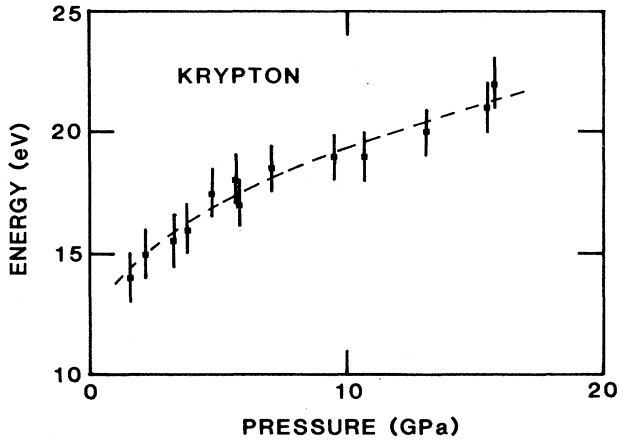

FIG. 8. Position of the second peak of the XANES part of the spectrum (origin of the energy is taken at the threshold energy) as a function of pressure. Dashed line is only a guide for the eyes.

body forces. It does not mean that all the properties of solid krypton may be reproduced with pair potentials; it has been shown,[7] that both equation of state and elastic properties cannot be simultaneously reproduced with a unique pair potential. It is necessary to introduce three-body exchange interactions.

Another remarkable feature appears in the spectra of Fig. 5; the near-edge part of the absorption spectra shows a double-peak structure. The peak at the right-hand side of the white line exists even at low pressure where the Debye-Waller factor is important enough to smear out the EXAFS oscillations above 40 eV. Its position in energy is pressure dependent (Fig. 8) and, within the precision of the measurements, varies linearly with the lattice parameter. Our set of data provides useful information for deducing the density of the krypton bubbles formed after implantation in metals.[24–26] If the effective pressure inside the bubbles is less than 2.5 GPa at room temperature, x-ray diffraction will probably give no information, because of the thermal motion of the atoms. Information about the pressure and the density can be obtained by the analysis of the XANES spectrum.

CONCLUSION

Solid krypton has been studied as a function of pressure in a diamond anvil cell by x-ray absorption spectroscopy in the dispersive mode. The analysis of the EXAFS part of the spectrum (i) gives an equation of state in good agreement with previous x-ray diffraction measurements, and (ii) allows one to compute the pressure dependence of the Debye-Waller factor. This coefficient decreases by a factor 3 when the pressure is increased by 10 GPa. The high value of σ^2 at low pressure explains why no EXAFS oscillations nor an x-ray diffraction peak were observed below 2 GPa.

Finally, the analysis of the XANES part of the spectrum shows the possibility of measuring pressure in bubbles of krypton implanted metals.

ACKNOWLEDGMENTS

The authors wish to thank J. M. Besson and P. Loubeyre for comments and discussions. This work was supported by the Institut National d'Astronomie et de Géophysique under Grant No. 83.70978 and the Commissariat à l'Energie Atomique under Grant No. 1617-A4. The Laboratoie de Physique des Milieux Condensés is Unité associée au Centre National de la Recherche Scientifique No. 782. The Laboratoire pour l'Utilisation du Rayonnement Electromagnétique is affiliated with CNRS, the Ministere de l'Education Nationale, and the Commisariat à l'Energie Atomique.

[1]D. Schiferl, R. L. Mills, and L. E. Trimmer, Solid State Commun. **46**, 783 (1983).
[2]K. Asaumi, Phys. Rev. B **29**, 7026 (1984).
[3]M. Ross, H. K. Mao, P. M. Bell, and J. A. Xu, J. Chem. Phys. **85**, 1028 (1986).
[4]A. P. Jephcoat, H. K. Mao, L. W. Finger, D. E. Cox, R. J. Hemley, and C. S. Zha, Phys. Rev. Lett. **59**, 2670 (1987).
[5]M. Grimsditch, P. Loubeyre, and A. Polian, Phys. Rev. B **33**, 7192 (1986).
[6]A. Polian and M. Grimsditch, Europhys. Lett. **2**, 849 (1986).
[7]A. Polian, J. M. Besson, M. Grimsditch, and W. A. Grosshans, Phys. Rev. B **39**, 1332 (1989).
[8]R. Ingalls, G. A. Garcia, and E. A. Stern, Phys. Rev. Lett. **40**, 334 (1978).
[9]R. Ingalls, E. D. Crozier, J. E. Whitemore, A. J. Seary, and J. M. Tranquada, J. Appl. Phys. **51**, 3158 (1980).
[10]J. P. Itié, M. Jeanlouis, E. Dartyge, A. Fontaine, and A. Jucha, J. Phys. (Paris), Colloq. **47**, C8-897 (1986).
[11]R. Münch, H. D. Hochheimer, A. Werner, G. Materlik, A. Jayaraman, and K. V. Rao, Phys. Rev. Lett. **50**, 1619 (1983).
[12]J. Röhler, J. P. Kappler, and G. Krill, Nucl. Instrum. Methods **208**, 647 (1983).
[13]E. Dartyge, C. Depautex, J. M. Dubuisson, A. Fontaine, A. Jucha, and G. Tourillon, Nucl. Instrum Methods A **246**, 452 (1986).
[14]H. Tolentino, E. Dartyge, A. Fontaine, and G. Tourillon, J. Appl. Cryst. **21**, 15 (1988).
[15]G. J. Piermarini, S. Block, J. D. Barnett, and R. A. Forman, J. Appl. Phys. **46**, 2774 (1975).
[16]H. K. Mao, P. M. Bell, J. W. Shaner, and D. J. Steinberg, J. Appl. Phys. **49**, 3276 (1978).
[17]See, for example, K. Ohsumi, S. Sueno, I. Nakai, M. Imafuku, M. Morikawa, M. Kimata, M. Nomura, and O. Shimomura, J. Phys. (Paris), Colloq. **47**, C8-189 (1986) [Fig. 1(a)].
[18]F. W. Kutzler, D. E. Ellis, T. I. Morrisson, G. K. Shenoy, P. J. Viccaro, P. A. Montano, E. H. Appelman, L. Stein, M. J. Pellin, and D. M. Gruen, Solid State Commun. **46**, 803 (1983).
[19]N. Kuroda, O. Ueno, and Y. Nishina, J. Phys. Soc. Jpn. **55**, 581 (1986).
[20]P. Eisenberger and G. Brown, Solid State Commun. **29**, 481 (1979).
[21]P. Loubeyre, D. Levesque, and J. J. Weiss, Phys. Rev. B **33**, 318 (1986).
[22]P. Loubeyre (private communication).
[23]R. A. Aziz and J. Slaman, Mol. Phys. **58**, 679 (1986).
[24]J. I. Budnick, D. M. Pease, M. H. Choi, Z. Tan, G. M. Hayes, F. Namavar, and H. C. Hayden, J. Phys. (Paris), Colloq. **47**, C8-1053 (1986).
[25]R. C. Bitcher and W. A. Jager, Nucl. Instrum. Methods B **15**, 435 (1986).
[26]J. H. Evans and D. J. Mazey, J. Phys. F **15**, L1 (1985).